Summary performance of the Estuary and Lake Computer Model (ELCOM): application in the Laurentian and other Great Lakes

Luis F. Leon, Jason P. Antenucci, Yerubandi R. Rao and Craig McCrimmon

ABSTRACT

The use of sophisticated three-dimensional (3D) hydrodynamic models is often required to simulate the spatial and temporal variability of water quality in large lakes. Recently, coupled lake–atmosphere models have also been developed to resolve the spatial distribution of the thermal behavior in lakes and to assess the feedback mechanisms at the air–water interface. In the studies summarized in this paper, the 3D Estuary and Lake Computer Model (ELCOM) acts as the hydrodynamic driver that provides temperature, salinity, and the transport fields that, if coupled with the Computational Aquatic Ecosystem Dynamics Model (CAEDYM), simulates nutrients, phytoplankton, zooplankton, and benthic habitat. This study presents a summary of the performance of ELCOM, and in an indirect form, serves as well as a corroboration of the strength or weakness of the coupled modeling and its ability to reproduce the thermal structure and circulation patterns, with examples from the Laurentian Great Lakes (Erie and Ontario), Northern Great Lakes (Great Slave Lake and Great Bear Lake), and Lake Winnipeg in Central Canada.

Key words | Great Bear Lake, Great Slave Lake, hydrodynamic model, Lake Erie, Lake Ontario

Luis F. Leon (corresponding author)
Yerubandi R. Rao
Craig McCrimmon
Environment Canada,
National Water Research Institute,
Burlington, Ont., L7R 4A6,
Canada
E-mail: *luis.leon@ec.gc.ca*

Jason P. Antenucci
Hatch Associates, Perth WA 6000,
Australia

Luis F. Leon
Department of Biology,
University of Waterloo,
Waterloo, Ont., N2L 3G1,
Canada

Jason P. Antenucci
Centre for Water Research,
University of Western Australia,
Crawley, WA 6009,
Australia

INTRODUCTION

Increasing concern over water quality in large lakes and the effects that climate change might have on them has required the application of coupled physical–biological numerical models as tools for understanding the relevant processes. One- and two-dimensional models (e.g., Lam *et al.* 1987; Boegman *et al.* 2008; Zhang *et al.* 2008) have commonly been used to analyze chemical, biological, and physical processes. A series of three-dimensional (3D) hydrodynamic models have been developed over the years (Lynch & Davies 1995), including the popular Princeton Ocean Model (POM; Blumberg & Mellor 1987). With the surge of available computational power at the desktop level, ecological modeling in lakes is increasingly being driven by sophisticated 3D hydrodynamic models, where complex ecological dynamic processes are linked to such models allowing simulation of water quality in large lakes (Imberger 1994; Dallimore *et al.* 2003).

Three-dimensional models have been used recently in the Great Lakes to simulate and analyze physical properties linked to water quality modeling. Schwab *et al.* (2009) used the vertically averaged dynamics from POM to analyze spatial and temporal patterns of phosphorus in Lake Erie. Specific process-based 3D-coupled biological and physical models have been developed for Lake Michigan (Chen *et al.* 2002; Ji *et al.* 2002). More recently, in Lake Erie, Leon *et al.* (2011) presented the capabilities of the Estuary and Lake Computer Model (ELCOM; Hodges & Dallimore 2006) and the Computational Aquatic Ecosystem Dynamics Model (CAEDYM; Hipsey & Hamilton 2006) as a coupled 3D hydrodynamic–biological model to capture the major circulation/thermal features and to simulate nutrient dynamics and phytoplankton distribution in the inland lakes.

The same modeling platform was used in a study in Lake Ontario, where algal fouling was causing blockages in the cooling water intakes at the Pickering nuclear station operated by Ontario Power Generation (OPG). The

doi: 10.2166/wqrjc.2012.022

ELCOM–CAEDYM models were used in this coastal area to help identify the role of nutrient dynamics and external conditions relevant to the recent resurgence of algae in the lake (Leon *et al.* 2012). In combination with extensive field sampling campaigns over 2 years (2007 and 2008), the study provided adequate information to validate the results of the numerical modeling exercise.

To study climate impacts, coupled lake–atmosphere models are also taking advantage of the capability of 3D models to resolve the spatial distribution of thermal properties in lakes. Recently, a few attempts have been made to couple 3D lake models with Regional Climate Models (RCM; Long *et al.* 2007). Their results show that fully coupled air–lake regional climate model systems provide reasonable temporal evolution of lake surface temperature and heat transfer at the air–lake interface in large lakes, allowing important feedbacks between the atmosphere, adjacent land, and the lakes at fine geographical scales. As part of the Global Energy and Water Cycle Experiment on the Mackenzie Basin (GEWEX-MAGS; Schertzer *et al.* 2008) detailed 3D hydrodynamic models were used to simulate the thermal structure on Great Slave Lake (Leon *et al.* 2007) and as part of the International Polar Year 2008 (IPY), similar models were used to assess the climate change impacts in Great Bear Lake (Rao *et al.* 2012).

Because all biochemical processes are temperature dependent, it is important that the models properly simulate the surface and sub-surface temperature structure in large lakes. Here we present a summary of the performance of the model and its ability to reproduce the thermal structure and circulation patterns in several large lakes. In particular, we show the ELCOM–CAEDYM model application in the lower Laurentian Great Lakes (Erie and Ontario); and with ELCOM as a stand-alone mode for the Northern Lakes (Great Slave Lake and Great Bear Lake) and in relatively shallower Lake Winnipeg in Central Canada. The model can be run either in isolation for hydrodynamic studies, or coupled with CAEDYM to simulate biological and chemical processes. It is worth noticing that when referring to ELCOM results, in particular from the thermodynamic component, but using the coupled version with CAEDYM, the latter is the prime modifier of the scalars being transferred back and forth between hydrodynamic and biochemical models. For instance, in ELCOM when in stand-alone mode, the extinction coefficient (which directly affects the thermal structure) is user-prescribed with constant values varied across the lake grid; but when coupled to CAEDYM, this parameter is one of the time-dependent scalars being transferred between the models for each cell in each time step. So in a novel form, the comparisons and summaries showed in the present exercise are also, in some indirect way, a corroboration of the strength of the coupled modeling framework as well.

METHODS AND MATERIALS

The results presented in this study are derived from the application of ELCOM as the 3D hydrodynamic model that predicts circulation, temperature, and salinity distribution in lakes subjected to external forcing, including wind, surface heating, and inflows. It was designed for modeling aquatic systems over short to seasonal time scales. ELCOM is a free surface, z-level model (Hodges & Dallimore 2006). The fundamental numerical scheme of ELCOM uses the grid stencil based on the Arakawa C-grid. The model solves the unsteady Reynold's averaged Navier–Stokes equations for incompressible flow using the hydrostatic assumption for pressure (Dallimore *et al.* 2003). Model forcing includes wind stresses, surface thermal gradients, inflows, outflows, rotational effects and even, if required for instance in estuaries, propagation of tidal water level through open boundary conditions. In all our study cases, the model was applied in lakes with closed boundaries. The hydrodynamic algorithms in the model are based on the Euler–Lagrange method for advection of momentum with a gradient solution for the free-surface height. It is unconditionally stable for purely barotropic flows. ELCOM's success at modeling internal wave fields is due to the use of a mixing layer model, improving estimation of stratification in a highly stratified lake, combined with a conservative flux-limiting scalar advection scheme (Hodges *et al.* 2000).

However, for stratified flows explicit discretization of the baroclinic terms in the momentum equation leads to a time step constraint based on the internal wave Courant–Friedrichs–Lewy (CFL) condition. Long-term preservation of lake stratification can be ensured by using a potential energy conserving filtering technique to counteract the accumulation of numerical dispersion. Some testing was done in Lake Erie with the energy filter, but a lack of meaningful response led us to eliminate the use of filters in subsequent runs and rely on other options, such as reducing the grid size, increasing the number of vertical layers, and/or reducing the modeling time step, to minimize the dispersion.

Reducing the grid size was abandoned early on due to the huge computational overload, compounded by the reduction in the time step forced by the higher resolution grid. As it currently stands, without parallel capabilities and in a fast machine – 3.6 GHz P4 processor – when tests were conducted using a 100 m grid resolution lake wide (with a time step of 30 s) the estimated running ratio of ELCOM alone was estimated to be 6:1 (taking 30 days to run the 6-month simulation period and four-folded when running coupled with CAEDYM for an estimated 4 months' running time).

General model setup

Over the last few years the ELCOM–CAEDYM model has been applied by the study group and others for hydrodynamic and water quality simulations in two of the Laurentian Great Lakes, Lake Erie and Lake Ontario (Leon *et al.* 2011, 2012; Paturi *et al.* 2012), and in Lake Winnipeg (Zhao *et al.* 2012); and related to climate impact studies in two northern lakes, Great Slave Lake and Great Bear Lake (Schertzer *et al.* 2003; Leon *et al.* 2007; Rao *et al.* 2012). In all cases, the model was configured with a 2×2 km horizontal grid resolution, 20 to 50 vertical layers, depending on depth and on the lake characteristics. Table 1 lists general information of the studied lakes and the model configuration with a 2 km grid. A general problem when modeling stratified flows is that temperature gradients are smoothed numerically, which leads to the phenomenon of numerical diffusion that ultimately translates into artificial heat dispersion for long simulations. By increasing the model vertical resolution and thereby reducing time step, this problem can be somewhat controlled to a certain extent in ELCOM, however at significant computational expense. In all cases, the dynamic qualitative behavior of the temperature structure was captured in profiles at different locations and surface output of mean circulation patterns, together with the spatial distribution of water surface temperatures.

Table 1 | Studied lakes' characteristics

Lake	Area (km^2)	Length (km)	Max depth (m)	Volume (km^3)
Great Bear Lake	31,080	373	446	2,236
Great Slave Lake	28,930	480	614	2,090
Lake Winnipeg	24,500	416	36 Narrows	294
Lake Erie	25,720	388	64	489
Lake Ontario	19,477	311	244	1,639

Lake Erie (1994, 2002, and 2005 simulations)

Lake Erie, extending from 41.5°N to 43.0°N and 79°W to 83.5°W, is the southernmost and shallowest of the five Laurentian Great Lakes (Figure 1), with a surface area of 25,700 km^2, a volume of 490 km^3 and a maximum depth of 64 m in the east region of the lake. It consists of three distinct basins on the basis of the bathymetry. The western basin (max depth 10 m) is separated from the relatively flat-bottomed central basin (max depth 25 m) by the Pennsylvania Ridge. The maximum depth of the Ridge at a point near the southern shoreline is 21 m. The physical characteristics of the lake and its basins have a major influence on such factors as the spatial variability in over-lake meteorological components, heat storage, water temperature distribution, circulation, and water level changes, etc. A major contribution of past hydrodynamic studies in Lake Erie has been to specify temperature, currents, and inter-basin fluxes of materials as needed for input to water quality and ecosystem models.

The first application of ELCOM in Lake Erie is described in Leon *et al.* 2005, where the hydrodynamic model results were compared with observed circulation patterns (Beletsky *et al.* 1999) and temperature profiles at sampling locations across the lake. Their results showed a good agreement between model and observations, thus offering the potential of exploring the 3D effects of nutrient dynamics. The model was further improved by increasing resolution and reducing the computational time step in later studies (Leon *et al.* 2006). In a subsequent application, ELCOM was coupled with CAEDYM to model the seasonal and spatial dynamics

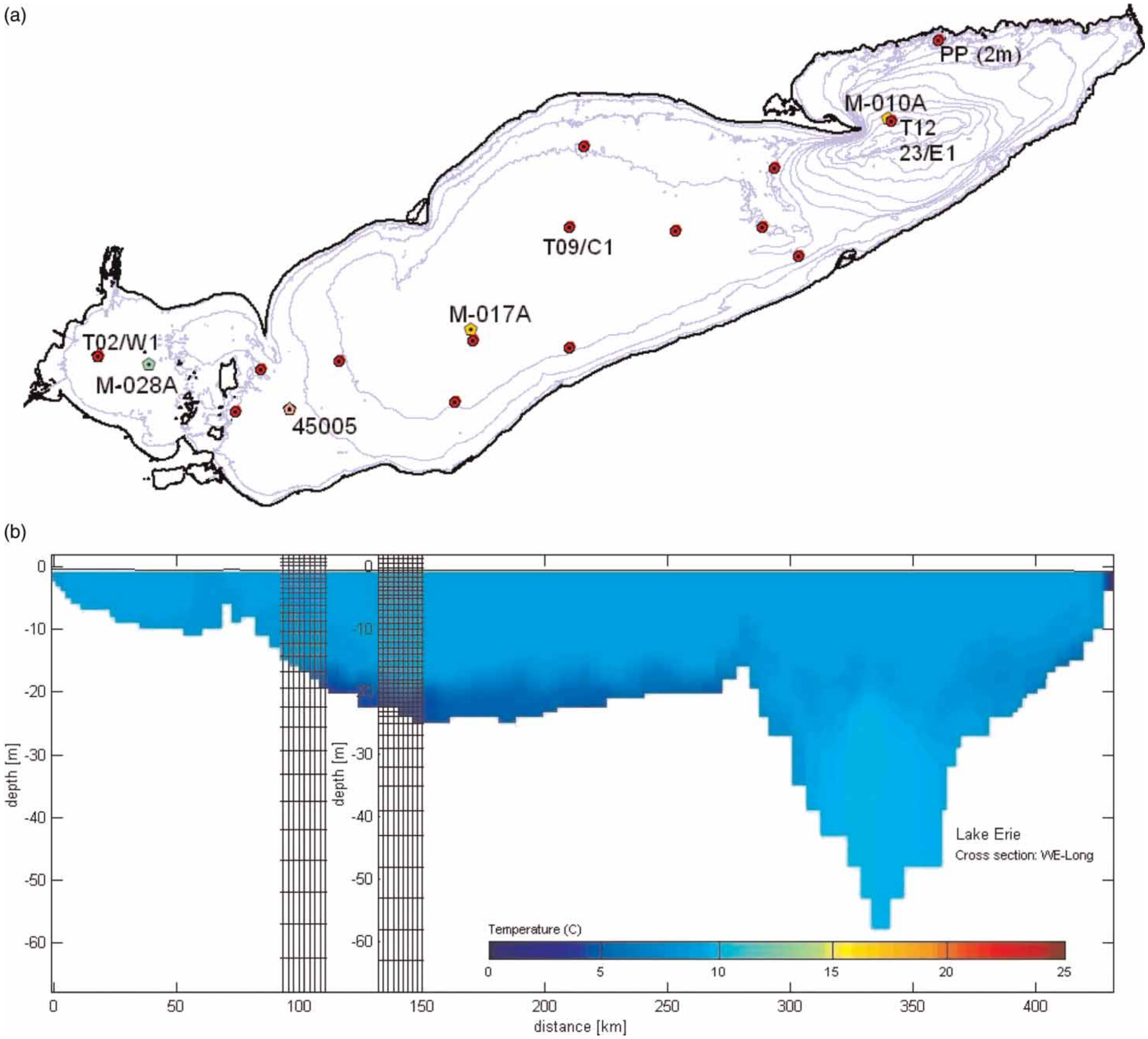

Figure 1 | Lake Erie: (a) mooring locations and meteorological stations (only sites and stations reported in the study are labeled) and (b) Lake Erie cross section showing the vertical model resolution (left grid – initial setup 30 vertical layers, right grid – increased layers to 45 with finer distribution in central basin).

of water quality and phytoplankton in Lake Erie (Leon *et al.* 2011). Recently, Lake Erie model was further tested with intensive measurements of the International Field Year on Lake Erie (IFYLE) (http://www.glerl.noaa.gov/ifyle/data/data.mooring.html) during 2005. To achieve finer resolution near the thermocline, the number of vertical layers was increased to 45 by adding more layers to the metalimnetic region (between the 15–20 m depth ranges, Figure 1(b)). The finer resolution around the thermocline and a reduced time step of 5 minutes reduced numerical dispersion, resulting in simulated thermal behavior better matching the observed data.

Lake Ontario (2004, 2005 lake-wide simulations and OPG 2007–2008 nearshore study)

Lake Ontario extends from 43.1°N to 44.3°N and 80°W to 76°W and has a surface area of 19,500 km² and a volume of

1,640 km^3. The mean depth is 86 m with a maximum depth of 245 m located in the southeast region (Figure 2). The downwind side of Lake Ontario is known to have high snowfalls due to lake effects. Compared to most other lakes, Lake Ontario has a wealth of archived meteorological and hydrographic data (Saylor *et al*. 1981). Furthermore, the lake has a rich history of studies using theoretical and numerical models (Simons 1974, 1975). More recently, Huang *et al.* (2010) applied three hydrodynamic models, namely POM, the Canadian version of Diecast model (CANDIE), and ELCOM. They compared these models with each other and with observations in Lake Ontario during 2006. Although they found all models provided basic characteristics of circulation and temperature, ELCOM predicted the vertical temperature structure more accurately.

The Lake Ontario study from 2007 to 2009 (Leon *et al.* 2012) focused on simulating major water quality variables that are important to nuisance algae growth at OPG water intakes off Pickering. Algal fouling, a serious problem along Great Lakes coastlines, is difficult to diagnose due to spatial and hydrodynamic variability in the nearshore zones. A nested approach was utilized, where lake-wide simulations at a 2 km grid resolution provided the boundary conditions for a higher resolution (100 m grid) model of the coastal segment of the lake in the vicinity of the Pickering nuclear power station. The initial setup for the model with a 2 km grid was done in the early stages of the project. Validation runs were successfully performed for the years 2004 and 2005.

For the nearshore high resolution simulations, more intensive data were collected in the coastal area of the Pickering station by partnering agencies and in combination with water quality extensive field sampling campaigns over 2 years, 2007 and 2008, provided invaluable information to validate the results of the model. The nested approach (Leon *et al.* 2012) included comparisons between results from the lake-wide simulations and simultaneously with the nearshore deployments. Two of the seven thermistor chains in the study were located in offshore waters (deeper than 25 m). Figure 2 shows the mooring sites and buoys used in the model.

Great Slave Lake (CFCAS study)

Located in the Mackenzie River Basin within Canada's northern climatic system (latitude 61°N) the Great Slave Lake (GSL) was studied from the perspective of its current base climate condition and potential climate changes in the region, as part of a research study conducted through the Global Energy and Water Cycle Experiment on the Mackenzie Basin (GEWEX/CFCAS; Schertzer *et al*. 2003). This lake is the fourth largest freshwater lake in Canada and the 12th largest lake in the world. It has a surface area of 21,000 km^2, maximum depth of 615 m (in the eastern arm) and a volume of 2,000 km^3 (Schertzer *et al.* 2008). As the weather and climate models interface with the lake model through the surface temperature and heat

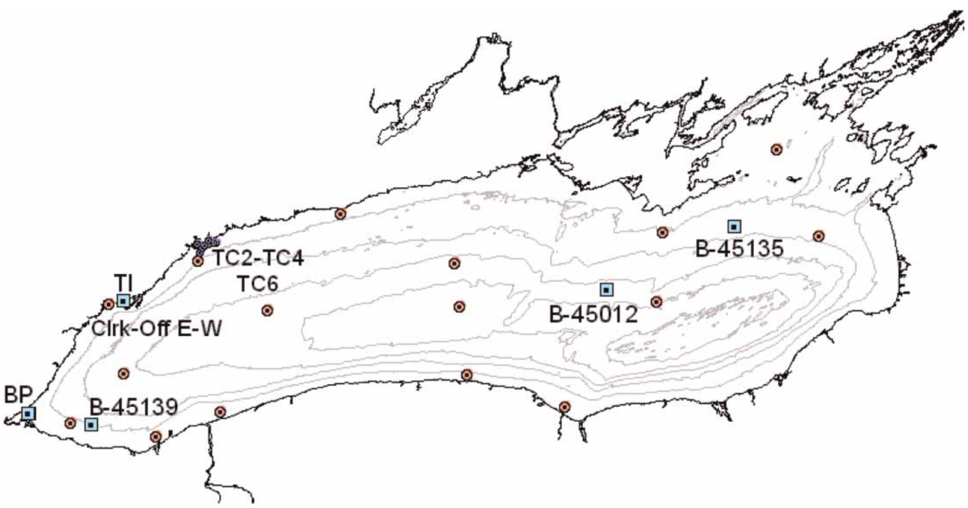

Figure 2 | Lake Ontario: mooring locations and meteorological stations.

fluxes, the accurate prediction of the in-lake thermal structure is of importance to the consistency in the air–water physical processes and to applications in studying weather and climate impacts on lake water quality and ecosystems. In particular, the heat content of the lake will be significantly affected by the thermal structure and thereby affect the weather and climate predictions.

With respect to the physical data, the depth values for a 2 km grid were extracted by superimposing the mesh on the polyconic projection of the Great Slave Lake (Schertzer *et al.* 2008). The model was set up with this bathymetry and 30 vertical layers. The setup excluded the complex island formation and deepest eastern portion of Christie arm and focused on the main central portion lake basin where the maximum depth is approximately 90 m. Observations, supporting this investigation included meteorology, radiation. and currents from the summer field program July to mid-September, 2003. Vertical temperature structure was observed at five thermistor chain moorings (sites labeled 1, 4, and 5 in Figure 3). During the evaluation of the performance of ELCOM on Great Slave Lake, model simulations showed dominant circulation patterns that can create relatively large spatial and temporal gradients in temperature (Leon *et al.* 2007). From the study, simulated temperatures compared well with cross-lake temperature observations both at the surface and vertically. Sensitivity analysis was applied to determine the critical meteorological variables affecting simulations of temperature and surface heat fluxes.

Great Bear Lake (Polar Year study)

Application of ELCOM on the Great Bear Lake (GBL) was a part of an International Polar Year (IPY), a large multidisciplinary, international scientific and social research program, with the objective of determining the present environmental status of the polar lake by quantifying its

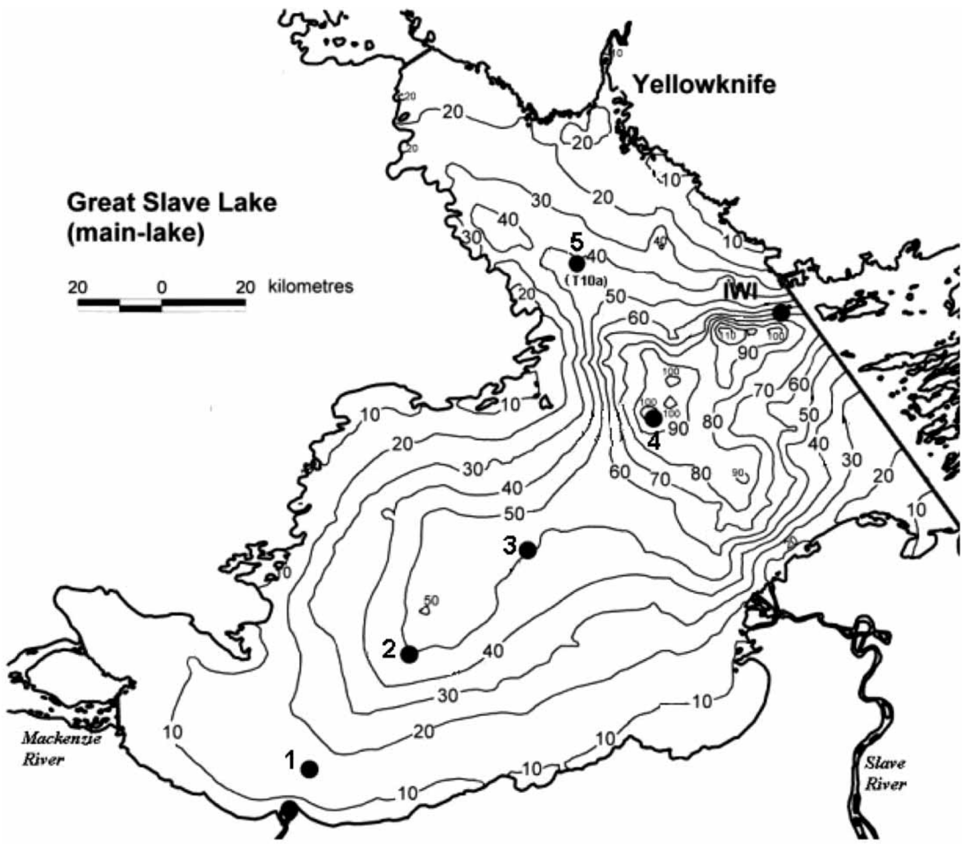

Figure 3 | Great Slave Lake: mooring locations and meteorological stations.

spatial and temporal variability and the potential effects due to climate change. To analyze the effect of climate on the temperature structure and heat fluxes on such a large polar lake, the project included a field program during two seasons in 2008 and 2009 to measure meteorology, heat fluxes, and physical limnological components and to model the temperature and currents for the measured conditions. GBL has a surface area of 31,000 km^2, maximum depth of 448 m and a volume of 2,200 km^3 (Rao *et al.* 2012). Meteorological measurements and solar radiation fluxes were measured at Deline (M1) and on Lionel Island (M2). A total of three summer temperature moorings were deployed in the Keith Arm (L1, L2, L3; Figure 4). Great Bear Lake is covered with ice from late November to July. Currently, the lake has an ice-free period of ~3–4 months.

Recently, an ice component has been integrated in ELCOM (Oveisy *et al.* 2012) which will open up the option of winter and multi-year simulations. For the purpose of this summary, and because at the time of the modeling work ELCOM did not had an ice component integrated, the simulations in GBL were only performed during the ice-free period (August 1 to September 30). The model had a similar setup as in the previous studies, using a 2 km grid bathymetry, 45 vertical layers and used the 2008 meteorological forcing and mooring data collected during the field campaign.

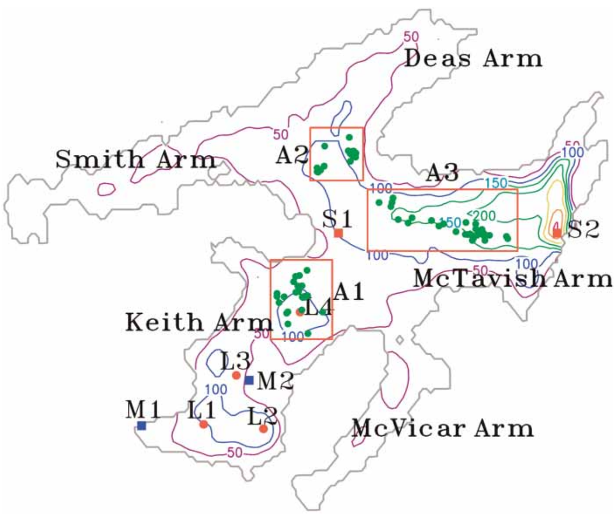

Figure 4 | Great Bear Lake: mooring locations and meteorological stations (only sites in Keith Arm are reported in the study).

Lake Winnipeg (Lake Winnipeg Basin Initiative, 2007–2012)

Lake Winnipeg is the 10th largest freshwater lake in the world and the fifth largest in Canada. It has two distinct basins, the North Basin (100 km wide) and the South Basin (40 km wide), which are separated by a 2.5 km wide channel. The dual-basin lake is elongated in shape, extends 436 km from north to south, and is relatively shallow with a mean depth of 9 and 12 m in South and North Basins, respectively. The Red, Winnipeg, and Saskatchewan Rivers are the major rivers flowing into Lake Winnipeg, contributing more than 70% of the water received. The lake drains northward into the Nelson River into Hudson Bay. As part of the Lake Winnipeg Basin Initiative (LWBI), a collaborative program between federal and provincial governments,

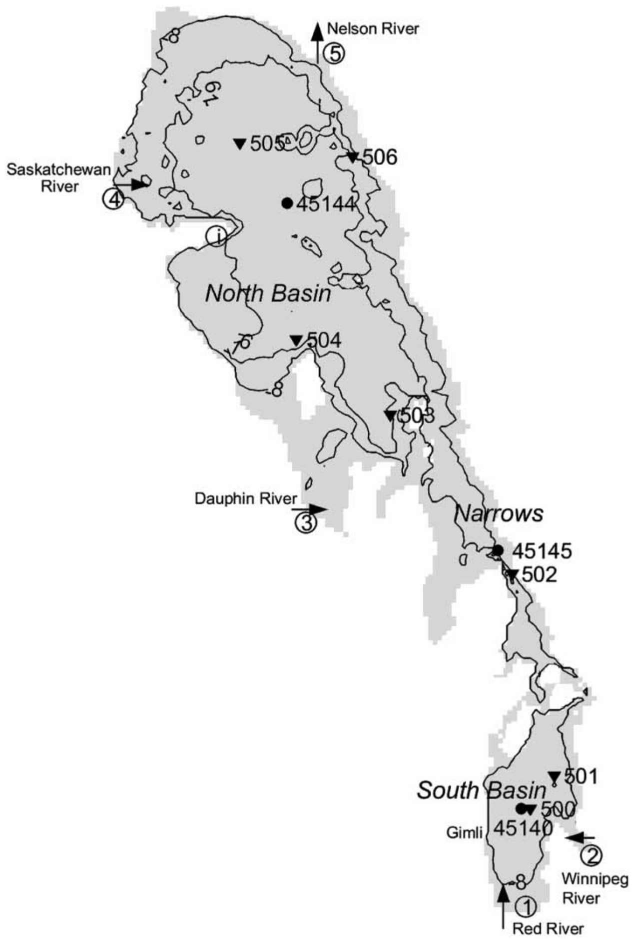

Figure 5 | Lake Winnipeg: mooring locations and meteorological stations.

both field data collection and numerical model development were carried out in Lake Winnipeg.

During 2007, currents, water temperature, wind, solar radiation, water levels, waves, and some water quality parameters at fixed mooring stations in the South and North Basins and in the Narrows were measured. There were six temperature moorings and three Acoustic Doppler Current Profiler (ADCP) measurements in the lake (Figure 5). Water level data were only collected at a station in the North Basin. However, water level gauges operated by Water Survey of Canada provided data at some coastal stations. ELCOM was applied to examine the 3D water circulation, temperature structures, and water levels in Lake Winnipeg. The computations were performed on a horizontal grid of 2 × 2 km. The bathymetry was derived from Canadian Hydrographic Service Charts with a mean lake level of 217.44 m. There were 21 levels in the vertical dimension with 1 m resolution for properly simulating temperature distribution. A time step of 5 minutes was found to be adequate for obtaining numerical stability. Simulations were started from rest, with horizontal free surface and isopycnals. Bottom and side land boundaries were modeled using the turbulent benthic boundary layer which accounts for most of the drag in the system.

RESULTS AND DISCUSSION

Faced with the challenge to select fair comparisons of model results, we focus the profile comparisons on a limited number of mooring locations. The statistics presented in Table 2 were compiled for the different lakes and periods described above, but selecting mainly the 2 km grid resolution and 20–45 vertical layers' setting. Simulations in the various studied lakes appeared to perform quite well. R^2 values ranged from 0.67 to 0.96. As correlations tend to give good fit for time series that shadow each other and produce decent regressions anyway, the Nash–Sutcliffe coefficient (NS; Nash & Sutcliffe 1970) was used as an additional performance test. For the same

Table 2 | Model and observed temperatures and performance statistics

Lake (output; case)	Site (depth)	Modeled Avg [min–max]	Observed Avg [min–max]	R^2	NS
Erie 1994 (semi-daily)	W1 (10 m)	20.5 [11.3–25.0]	20.7 [11.3–25.1]	0.96	0.85
	C1 (25 m)	18.1 [6.2–23.3]	18.7 [6.3–24.8]	0.96	0.85
	E1 (60 m)	16.8 [4.8–23.4]	17.4 [3.25–23.8]	0.95	0.83
Erie 2002 (semi-daily)	Peacock (2 m)	17.1 [8.0–23.9]	17.1 [7.2–24.2]	0.78	0.68
	East 23 (58 m)	15.7 [2.5–25.1]	15.7 [3.1–25.2]	0.98	0.88
Erie 2005 (semi-daily; 30 v)	W-T05*(10 m)	20.8 [15.4–26.6]	23.4 [14.7–26.7]	0.84	0.73
	E-T12 (58 m)	17.5 [4.4–25.3]	18.3 [3.4–25.7]	0.96	0.84
Erie 2005 (semi-daily; 45 v)	W-T05*(10 m)	20.7 [15.0–26.6]	23.4 [14.7–26.7]	0.83	0.77
	C-T09 (22 m)	19.3 [6.4–25.4]	20.1 [5.8–26.4]	0.93	0.81
	E-T12 (58 m)	17.7 [4.4–25.1]	18.3 [3.4–25.4]	0.96	0.85
Erie 2005 (semi-daily; 1 km)	W-T05*(10 m)	20.7 [15.0–26.5]	23.4 [14.7–26.7]	0.86	0.63
	E-T12 (58 m)	17.7 [9.9–25.1]	18.3 [3.4–25.4]	0.96	0.85
Ontario 2004 (daily) layer = 18 m	$\text{Clark}_{\text{intake}}$ (21 m)	12.3 [4.4–19.5]	12.4 [5.3–20.8]	0.83	0.81
layer = 10 m	OffE (24 m)	13.8 [5.0–19.4]	13.8 [5.3–21.4]	0.74	0.73
Ontario 2007 (semi-daily)	TC2 (25 m)	13.4 [4.3–22.5]	15.1 [5.6–24.0]	0.67	0.55
	TC4 (15 m)	14.6 [6.4–24.1]	14.7 [5.9–22.8]	0.71	0.73
	TC6 (15 m)	15.6 [6.5–25.3]	15.3 [5.3–23.8]	0.73	0.69
Great Slave 2003 (semi-daily)	#1 (T06A-15 m)	13.1 [3.1–19.7]	12.9 [6.3–19.1]	0.83	0.59
	#4 (T01A-90 m)	7.3 [2.4–12.2]	7.9 [2.2–14.9]	0.87	0.76
	#5 (T10A-40 m)	9.4 [2.3–15.5]	9.8 [2.0–16.9]	0.93	0.89

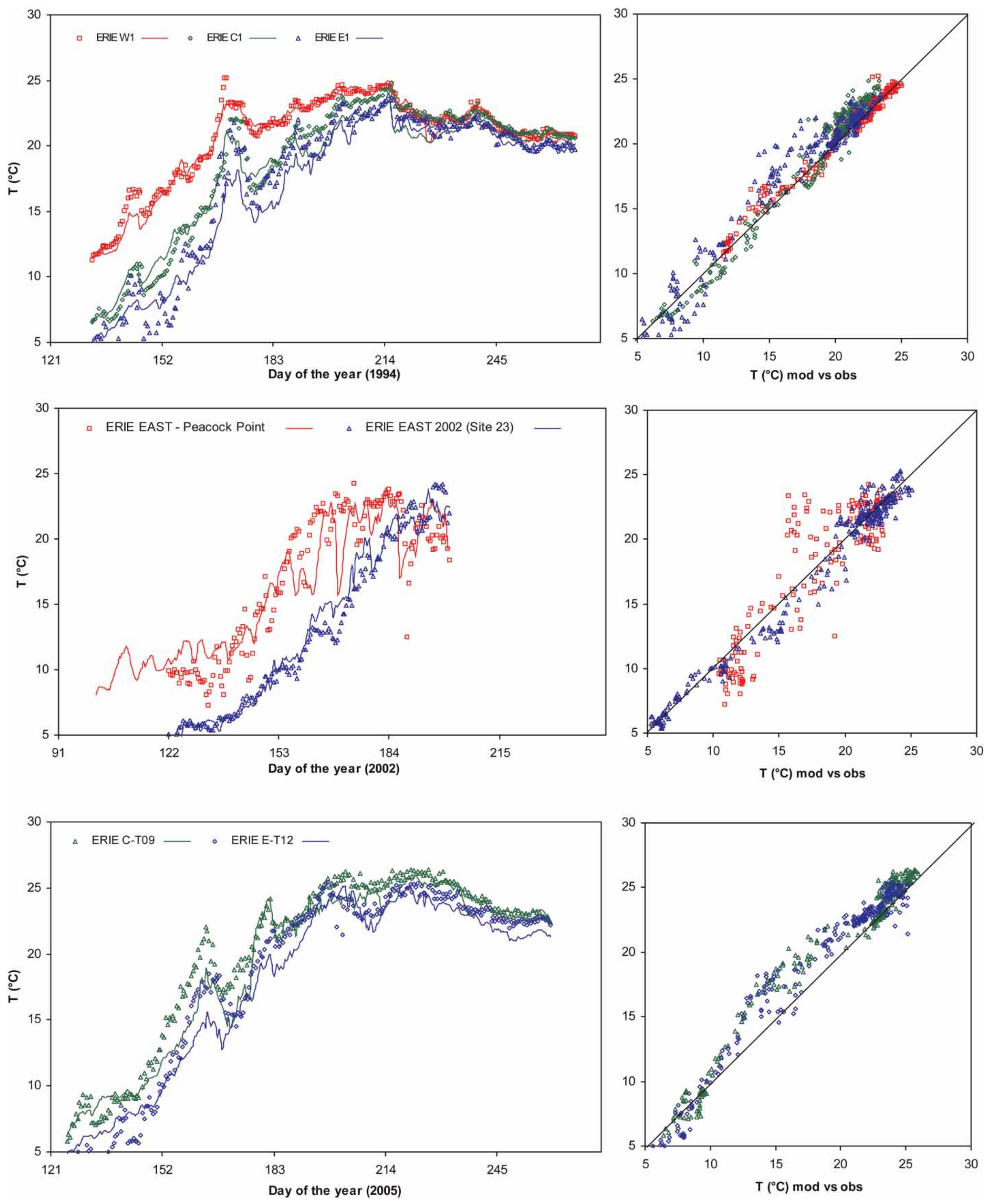

Figure 6 | Lake Erie time series of semi-daily temperature comparisons at selected thermistor chain sites (from top to bottom 1994, 2002, and 2005 simulations). Note: in all the 45° correlation [x = mod, y = obs] plots the trend line intersects origin.

sites NS values ranged from 0.55 to 0.89; NS > 0.4 are considered to be satisfactory (good above 0.75 and 1.0 indicating a perfect fit).

Lake Erie results are by far the most abundant due to being the first of the Great Lakes to be simulated with ELCOM, and due to the amount of available data to test

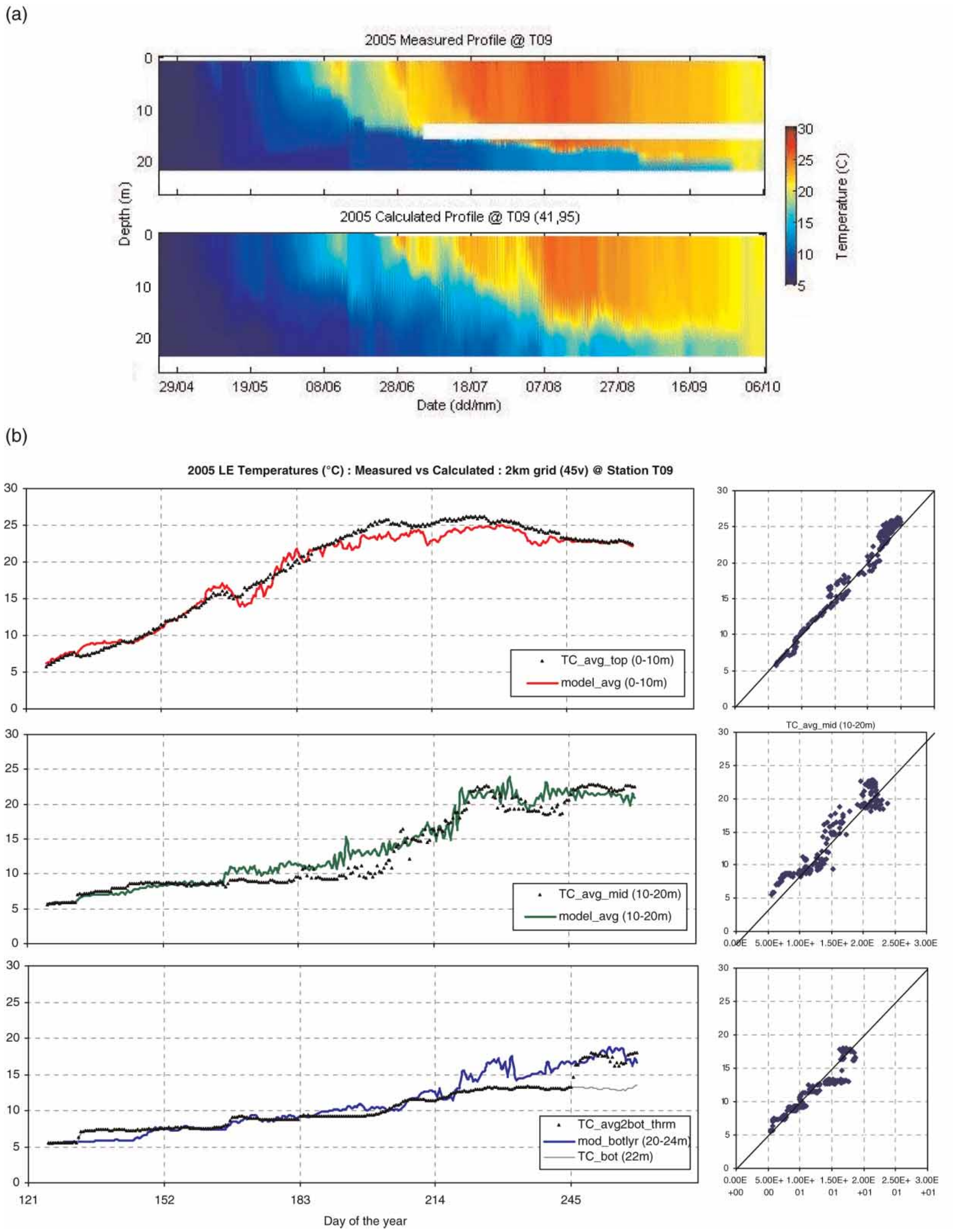

Figure 7 | (a) Simulation and observed profile for Lake Erie in 2005: 2 km grid/45 v layers T09 at central basin and (b) temperature time series **Station 09** (top, middle, and bottom layers). Note: in all the 45° correlation [x = mod, y = obs] plots the trend line intersects origin.

the model. The initial comparative work involved simulations for 1994 where data were available from three deployed moorings, one for each basin (W1, C1, E1; Figure 1). In 2002, additional thermistor chains were used near Peacock Point as well as the offshore deep station (PP, #23; Figure 1). During 2005, being IFYLE, there was benefit from more intensive instrumentation and sites T9 and T12 were selected for comparisons mostly for the central and east basins. Figure 6 shows the modeled and observed temperature (at 2 m depth) for the above sites and the 3 simulated years. Figure 7(a) presents the temperature profile at site T09. Figure 7(b) shows time series comparison of modeled and observed temperatures at different depth layers for the site T09 in the central basin.

In general, for Lake Ontario, the thermal structure was properly modeled for the 2004–2005 simulations for temperature profiles in sites located in the west, central, and east regions of Lake Ontario. Results from the models were extracted to include these common locations as additional profile grid cells in both domains. Figure 8 shows the comparison between measured and calculated profiles for TC1 and TC2 (the two offshore sites). As before, the model was considered to perform well and the evident presence of upwelling of cold water was fairly reproduced in the model.

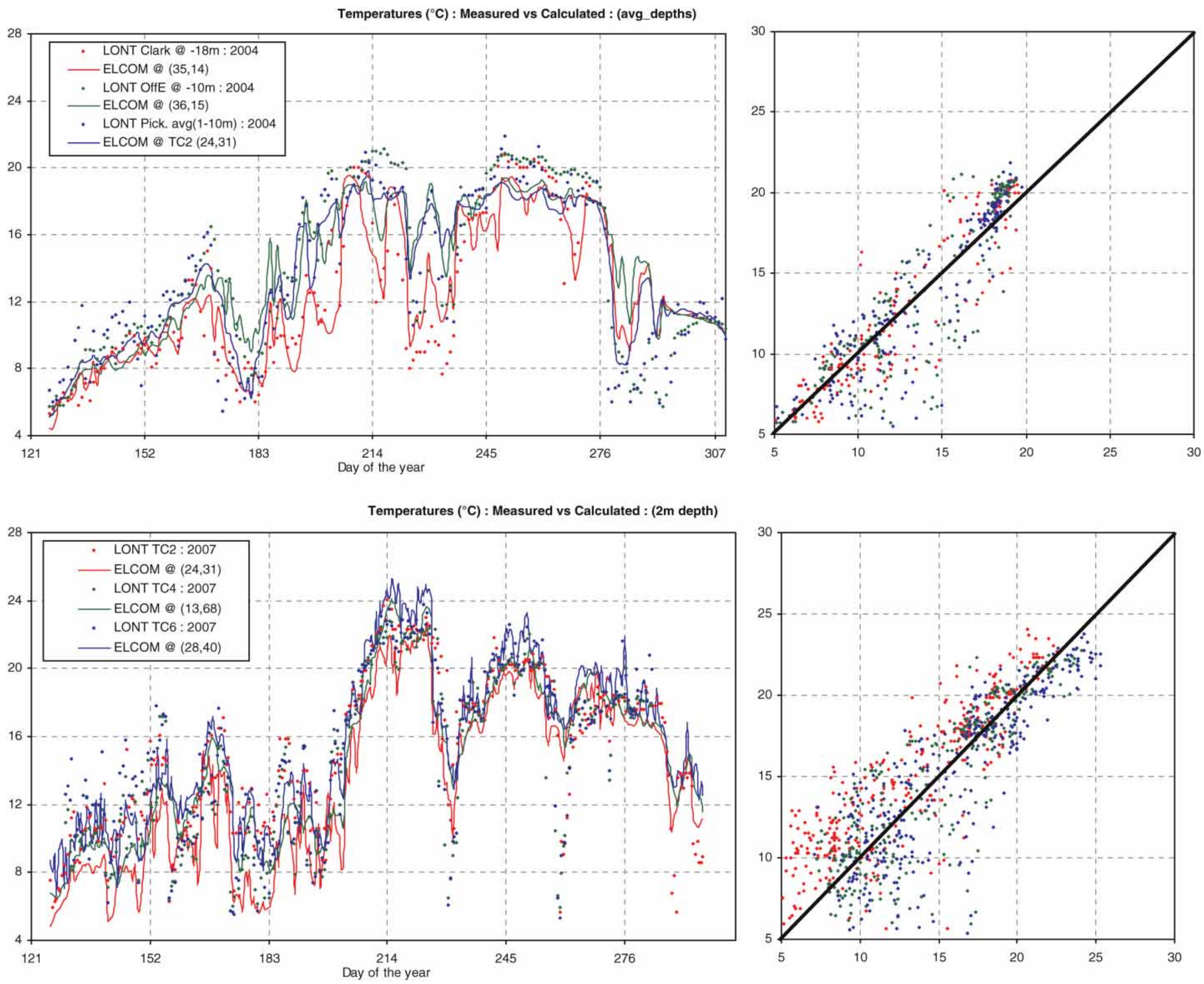

Figure 8 | Lake Ontario daily averages profiles at selected thermistor chain sites for 2004 and 2007 simulations. Note: in all the 45° correlation [$x = $mod, $y = $obs] plots the trend line intersects origin.

For Great Slave Lake, Figure 9 shows the temperature time series for the sites T01a, T06a, and T10a (Figure 3). The results show that the simulated values conform with those observed in terms of the spatial gradient from near-shore to offshore. These and the results discussed earlier indicated the consistency in the computed and observed temperature; the results showed the warming of the upper layer in July with some cooling events happening early in August and September, due to wind storms and cooler air temperatures. Table 2 presents, for the stations, a comparison of the average percentage differences and basic statistics between modeled and measured top layer temperatures over the stratified period (July–September 2003).

In Great Bear Lake, the observations (Figure 10), during the brief summer, show that the Keith Arm is isothermal (<4 °C) until day 227 and weak stratification formed later. However, station L3 warmed up much earlier because of its shallow depth. In the main lake, the water column appears to be isothermal and less than 4 °C throughout the period except for brief warming on days 248 and 254. Therefore, as in temperate lakes (e.g., Rodgers 1987; Rao *et al.* 2004) a thermal bar develops in Great Bear Lake dividing the stratified shallow areas of the lake from the unstratified deeper regions. Although the strength of the stratification (thermocline) is not strong, it is deeper in shallow areas (Stn L3) compared to those in the deep water region (Stns L1 and L2). The dominant features of the thermal structure are reasonably well captured by the model.

In Lake Winnipeg, the time–depth distributions of simulated temperatures were compared with observed temperatures at stations in the South Basin, Narrows, and the North Basin (Figure 11). The ELCOM model captured the dominant features of evolving thermal structure of the water column well. The shallow South Basin warmed quickly and remained isothermal for most of the study period (Figures 11(a) and 11(d)). The water temperature was isothermal in the Narrows (Figures 11(b) and 11(e)). Stratification was only observed in the deeper North Basin in late June, but it vanished rapidly by the end of July, due to high wind occurring during this period (Figures 11(c) and 11(f)). Comparisons of the model results with the field observed temperatures demonstrated that the model can accurately depict the observed thermal structure at all stations.

We also assessed ELCOM performance in reproducing the water levels and the depth mean currents in the lake. In contrast to the previous statistics, in the Lake Winnipeg project, we measured the model performance in terms of the γ^2 value, which is defined as the variance of the model errors (differences between the observations and model results) normalized by the observed variance: $\gamma^2 = Var\ (\mathrm{O} - \mathrm{M})/Var(\mathrm{O})$, where O and M are the observed

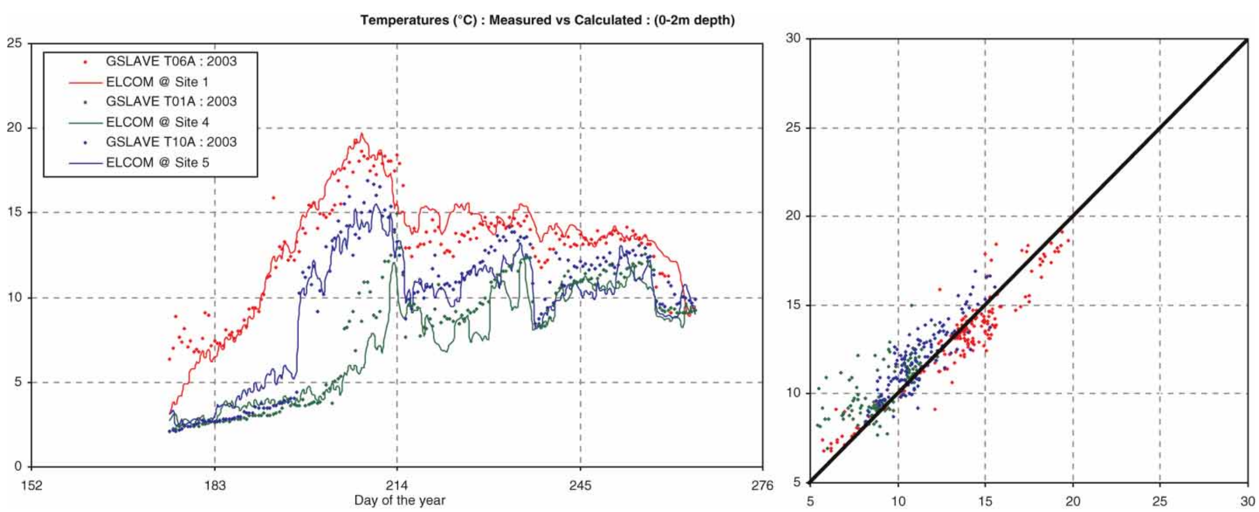

Figure 9 | Great Slave Lake: 2003 temperature time series at sites T01a, T06a, and T10a. Comparison between computed average surface temperatures (top layer) with measured temperatures (average 0–2 m depth).

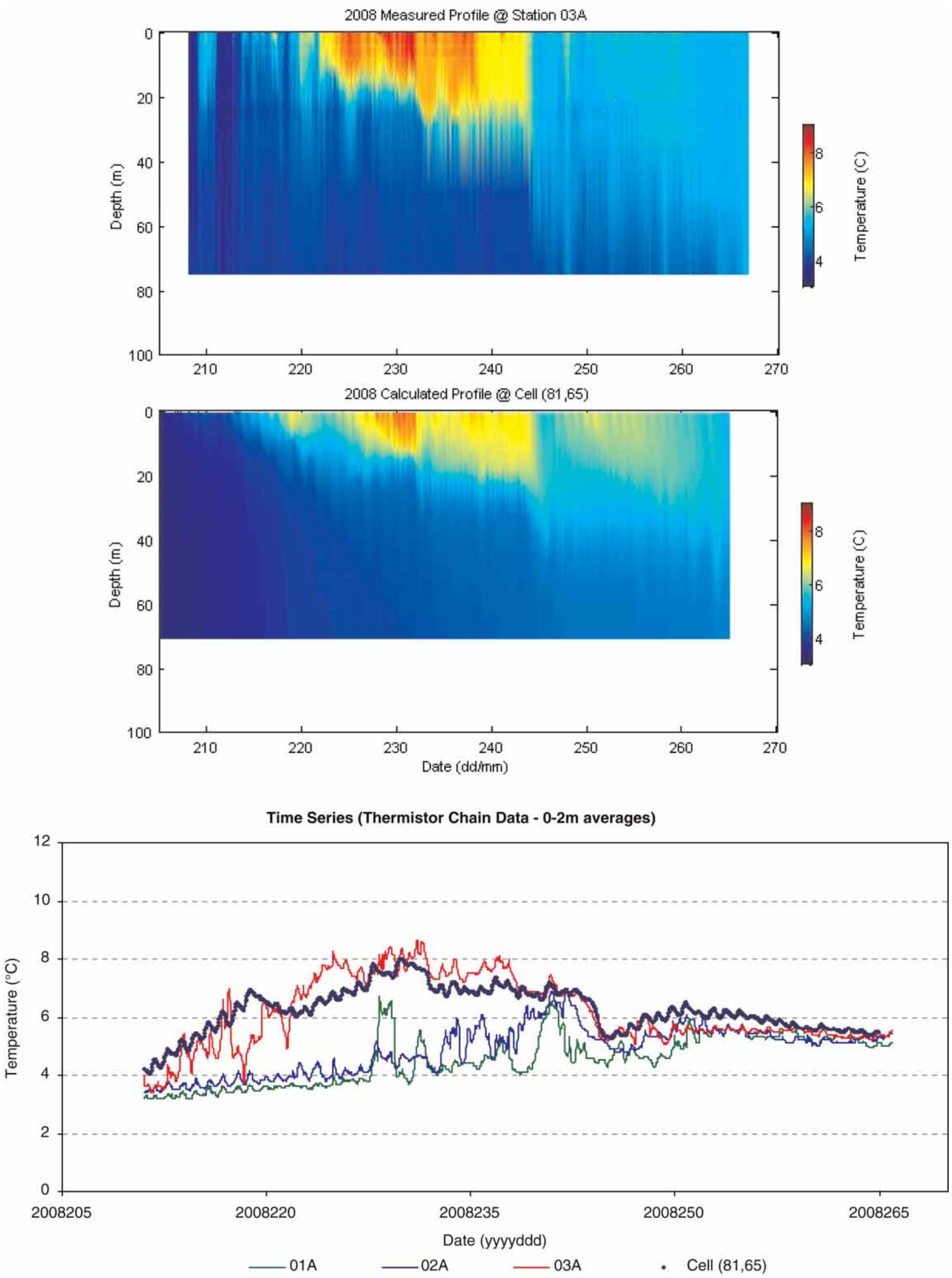

Figure 10 | ELCOM temperature simulation in Great Bear Lake in 2003 (top) and time series at selected sites (bottom).

and model calculated variables, respectively, and *Var* is the variance (Thompson & Sheng 1997). The γ^2 value is a measure of the variance of the model error upon the variance of the observations. The smaller the γ^2 is, the better the model results fit the observations. The simulated water levels at two sites (station in the North Basin and a station in the Narrows) agreed reasonably well with the observations, with γ^2 values of about 0.356 at station 506 and

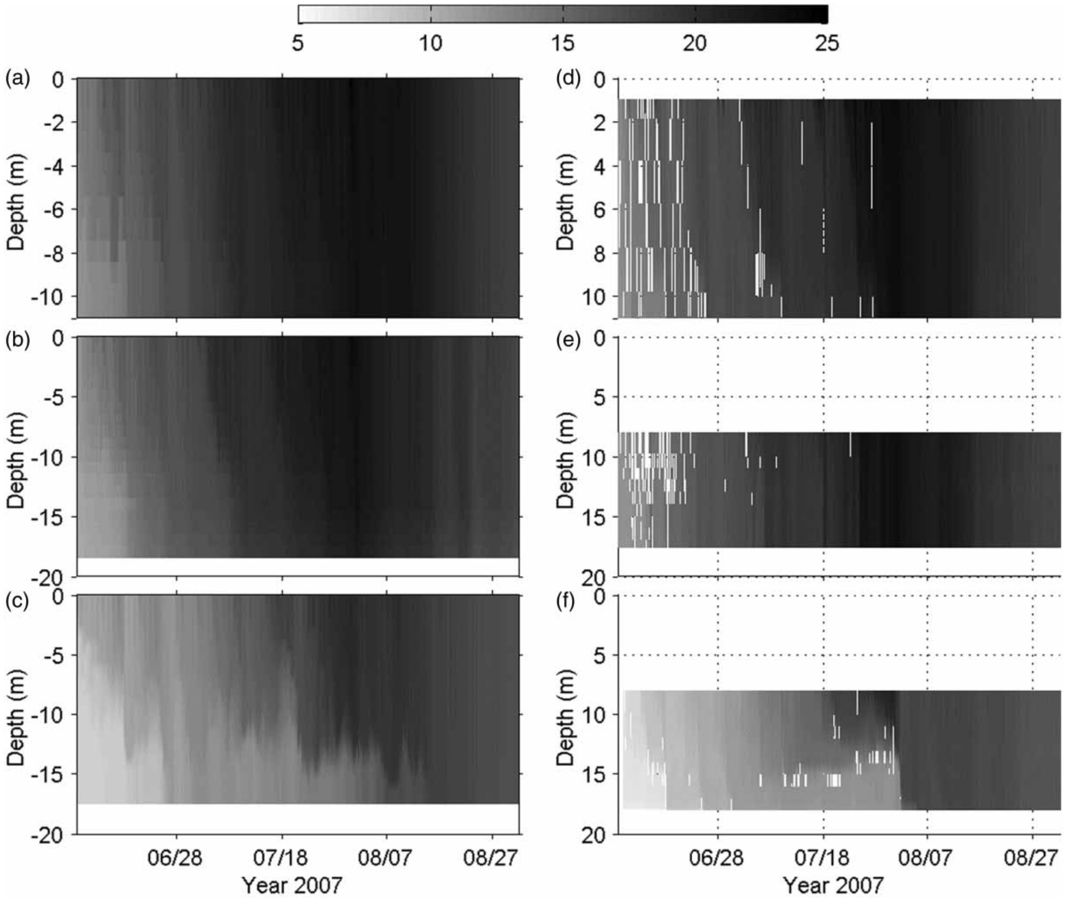

Figure 11 | Lake Winnipeg temperature profiles (a), (b), (c) modeled and (d), (e), (f) measured.

0.397 at station 502. ELCOM simulates water level very well during calm periods, but underestimates the storm surges and surface seiches during storm events, which could be because of coarse horizontal resolution and uniform basin winds in the model.

CONCLUSIONS

The 3D hydrodynamic model ELCOM was successfully applied to several large lakes in Canada. The model captured the dominant features of evolving thermal structure of the water column in all lakes. In particular, the model has been successful in predicting the sharp structure of the thermocline in Lake Erie. The model produced circulation and thermal characteristics in shallower Lake Winnipeg are also very encouraging, and the assessment of the impact of climate change in the northern lakes also provided good results. In order to gain a general understanding of the model abilities and in an attempt to go beyond the above subjective characterization of the results, this summary provides a measure of the performance of the model on the different studied lakes and under very different forcing conditions. The statistics and coefficient of efficiency (NS) for all lakes indicates that the model performs at the level denoted as excellent agreement between predictions and observed values (values above 0.4 are considered to be a fair model representation and the lowest value reported is in the range of 0.56).

In general, it can be concluded that the thermal structure is predicted reasonably well in all the lakes but some differences between deep sites and shallow areas are evident. The model appears to produce better results when comparing deeper sites, where the effect of the differences along the thermocline yields a lesser impact on the overall prediction. The case of the offshore site in Lake Ontario where the reported NS is lower than for other similar offshore sites, is due to the fact that its depth of 25 m coincides pretty much with the thermocline depth, also the vicinity with the shore line makes this region quite energetic and when rapid upwelling occurs, the model fails to keep track of the steep gradient to catch up to the temperature peak. If a 3-hour moving average is used on the temperature series instead of hourly, the model NS increases its value to a range consistent with the rest of the offshore sites.

Although not discussed in detail, the numerical model was also used to study the biochemical process occurring in many of these lakes. These model projections provide some preliminary understanding of mixing and transport of material from various sources, which include rivers, sewage treatment plants, etc. In the lower Great Lakes water quality components were also simulated by coupling with CAEDYM to examine the ecosystem response under different nutrient loading conditions. Currently, CAEDYM is being further improved by including location-specific concerns such as recent infestation of zebra and quagga mussels and *Cladophora* in the Great Lakes. Therefore, we believe that the ELCOM–CAEDYM model is expected to be a useful tool for water quality modeling and water resources management of large lakes in Canada.

ACKNOWLEDGEMENTS

We thank the Centre for Water Research, University of Western Australia for providing access to the ELCOM model. We thank Environment Canada's Research Support Branch for providing field work assistance. Several individuals participated during the course of this project; in particular we would like to thank William M. Schertzer, David C. Lam, Ralph Smith, and David Swayne in the guidance for ELCOM applications in Canadian lakes. Financial support came from Ontario Power Generation, NSERC, Environment Canada and partners such as Ontario Ministry of Environment.

REFERENCES

Beletsky, D., Saylor, J. H. & Schwab, D. J. 1999 Mean circulation in the Great Lakes. *J. Great Lakes Res.* **25** (1), 78–93. 70718-5.

Blumberg, A. & Mellor, G. L. 1987 A description of a three-dimensional coastal ocean circulation model. In: *Three-Dimensional Coastal Ocean Models* (N. S. Heaps, ed.). American Geophysical Union, Washington, DC, pp. 1–16.

Boegman, L., Loewen, M. R., Culver, D. A., Hamblin, P. F. & Charlton, M. N. 2008 Spatial dynamic modeling of algal biomass in Lake Erie: Relative impacts of dreissenid mussels and nutrient loads. *J. Environ. Eng.* **134**, 456–468.

Chen, C., Ji, R., Schwab, D. J., Beletsky, D., Fahnenstiel, G. L., Johengen, T. H., Vanderploeg, H., Eadie, M., Jiang, B., Bundy, M., Gardner, W., Cotner, J. & Lavrenty, P. J. 2002 A model study of the coupled biological and physical dynamics in Lake Michigan. *E. Model.* **152** (2–3), 145–168.

Dallimore, C. J., Hodges, B. R. & Imberger, J. 2003 Coupling an underflow model to a 3D hydrodynamic model. *J. Hydraul. Eng.* **129** (10), 748–758.

Hipsey, M. R. & Hamilton, D. P. 2006 *Computational Aquatic Ecosystem Dynamics Model: CAEDYM, Science Manual v3.3*. Centre for Water Research, University of Western Australia, Perth, Australia.

Hodges, B. & Dallimore, C. 2006 *Estuary, Lake and Coastal Ocean Model: ELCOM Science Manual v2.2*. Centre for Water Research, University of Western Australia, Perth, Australia.

Hodges, B. R., Imberger, J., Saggio, A. & Winters, K. 2000 Modeling basin scale waves in a stratified lake. *Limnol. Oceanogr.* **45**, 1603–1620.

Huang, A., Rao, Y., Lu, Y. & Zhao, J. 2010 Hydrodynamic modeling of Lake Ontario: An intercomparison of three models. *J. Geophys. Res.* **115**, C12076.

Imberger, J. 1994 Transport processes in lakes: A review. In: *Limnology Now: A Paradigm of Planetary Problems* (R. Margalef, ed.). Elsevier Science, Amsterdam, pp. 79–193.

Ji, R., Chen, C., Budd, J. W., Schwab, D. J., Beletsky, D., Fahnenstiel, G. L., Johengen, T. H., Vanderploeg, H., Eadie, B., Cotner, J., Gardner, W. & Bundy, M. 2002 Influences of suspended sediments on the ecosystem in Lake Michigan: A 3-D coupled bio-physical modeling experiment. *Eco. Model.* **152**, 169–190.

Lam, D. C. L., Schertzer, W. M. & Fraser, A. S. 1987 A post-audit analysis of the NWRI nine-box water quality model for Lake Erie. *J. Great Lakes Res.* **13**, 782–800.

Leon, L. F., Imberger, J., Smith, R., Hecky, R., Lam, D. C. & Schertzer, W. 2005 Modeling as a tool for nutrient management in Lake Erie: A hydrodynamics study. *J. Great Lakes Res.* **31**(Suppl. 2), 309–318.

Leon, L. F., Lam, D. C., Schertzer, W. M., Swayne, D. A. & Imberger, J. 2007 Towards coupling a 3D hydrodynamic lake model with the Canadian Regional Climate Model: Simulation on Great Slave Lake. *J. Environ. Modell. Software* **22**, 787–796.

Leon, L. F., Smith, R. E. H., Hipsey, M. R., Bocainov, S. A., Higgins, S. N., Hecky, R. E., Antenucci, J. P. & Guildford, S. J. 2011 Application of a 3D hydrodynamic-biological model for seasonal and spatial dynamics of water quality and phytoplankton in Lake Erie. *J. Great Lakes Res.* **37** (1), 41–53.

Leon, L. F., Smith, R., Mailkin, S., Depew, D., Hipsey, M. R., Antenucci, J., Higgins, S. & Hecky, R. E. 2012 Nested 3D modelling spatial dynamics of nutrients and phytoplankton in Lake Ontario nearshore zone. *J. Great Lakes Res SpIss.* **385**, 171–183.

Leon, L. F., Smith, R. E. H., Romero, J. R. & Hecky, R. E. 2006 Lake Erie Hypoxia Simulations with ELCOM-CAEDYM. 3rd Biennial Meeting of the International Environmental Modelling and Software Society, IEMSs 2006, July 2006, Burlington, Vermont, USA.

Long, Z., Perrie, W., Gyakum, J., Caya, D. & Laprise, R. 2007 Northern lake impacts on local seasonal climate. *J. Hydrometeorol.* **8**, 881–896.

Lynch, D. R. & Davies, A. M. 1995 *Assessment for Coastal Ocean Models.* Coastal and Estuarine Studies, American Geophysical Union, Washington, DC, Vol. 47.

Nash, J. E. & Sutcliffe, J. V. 1970 River flow forecasting through conceptual models part I – A discussion of principles. *J. Hydrol.* **10** (3), 282–290.

Oveisy, A., Boegman, L. & Imberger, J. 2012 Three-dimensional simulation of lake and ice dynamics during winter. *Limnol. Oceanogr.* **57** (1), 43–57.

Paturi, S., Boegman, L. & Rao, Y. R. 2012 Hydrodynamics of eastern Lake Ontario and the upper St. Lawrence River. *J. Great Lakes Res.* **38**, 194–204.

Rao, Y. R., Huang, A., Schertzer, W. M. & Rouse, W. R. 2012 Modelling of physical processes and assessment of climate change impacts in Great Bear Lake. *J. Atmosphere-Ocean* **50** (3), 317–333.

Rao, Y. R., Skafel, M. G. & Charlton, M. N. 2004 Circulation and turbulent exchange characteristics during the thermal bar in Lake Ontario. *Limnol. Oceanogr.* **49**, 2190–2200.

Rodgers, G. K. 1987 Time of onset of full thermal stratification in Lake Ontario in relation to temperatures in winter. *Can. J. Fish. Aquat. Sci.* **44** (12), 2225–2229.

Saylor, J. H., Bennet, J. R., Boyce, F. M., Murthy, C. R., Picket, R. L. & Simons, T. J. 1981 Water movements. In: *IFYGL-International Field Year on the Great Lakes* (E. J. Aubert & T. L. Richards, eds). Great Lakes Environmental Laboratory, Ann Arbor, MI, pp. 7–32.

Schertzer, W. M., Rouse, W. R., Blanken, P. D. & Walker, A. E. 2003 Over-lake meteorology and bulk heat exchange of Great Slave Lake 1998 and 1999. *J. Hydrometeor.* **4** (4), 649–659.

Schertzer, W. M., Rouse, W. R., Blanken, P. D., Walker, A. E., Lam, D. C. L. & Leon, L. 2008 Chapter 11, Interannual variability of the thermal components and bulk heat exchange of Great Slave Lake. In: *Cold Region Atmospheric and Hydrologic Studies: The Mackenzie GEWEX Experience, Vol. 2: Hydrologic Processes* (M. K. Woo, ed.). Springer, New York, 507 pp.

Schwab, D. J., Beletsky, D., DePinto, J. & Dolan, D. M. 2009 A hydrodynamic approach to modeling phosphorus distribution in Lake Erie. *J. Great Lakes Res.* **35**, 50–60.

Simons, T. J. 1974 Verification of numerical models of Lake Ontario, Part 1: Circulation in spring and summer. *J. Phys. Oceanogr.* **4**, 501–523.

Simons, T. J. 1975 Verification of numerical models of Lake Ontario, Part 2: Stratified circulations and temperature changes. *J. Phys. Oceanogr.* **5**, 98–110.

Thompson, K. R. & Sheng, J. 1997 Assessing the predictive skill of a 3D barotropic model of subtidal current variability on the Scotian Shelf. *J. Geophys. Res.* **24**, 987–1003.

Zhang, H., Culver, D. A. & Boegman, L. 2008 A two-dimensional ecological model of Lake Erie: application to estimate dreissenid impacts on large lake plankton populations. *Ecol. Mod.* **214**, 219–241.

Zhao, J., Rao, Y. R. & Wassenaar, L. I. 2012 Numerical modeling of hydrodynamics and tracer dispersion during ice-free period in Lake Winnipeg. *J. Great Lakes Res.* **38** (Suppl 3), 147–157.

First received 2 January 2012; accepted in revised form 2 November 2012